

## Formation Evaluation of the Lower Cretaceous Nubian Formation, East Sirt Basin, Libya

[www.doi.org/10.62341/mafe3510](http://www.doi.org/10.62341/mafe3510)

Mouna M. A. Marghani and Abdulhadi Elsounousi Khalifa

College Engineering Technology-Janzour, Tripoli-Libya  
almarghnimona@gmail.com

### Abstract

It is crucial to gain a deeper comprehension of the factors that influence reservoir quality in low-porous heterogeneous reservoirs for the purpose of petroleum exploration and production. This research examines the depositional and post-depositional influences on the sandstone reservoir quality of the Upper Nubian Member in the North Gialo Field, East Sirt Basin, Libya. To explore the connection between facies and petrophysical parameters and to determine the impact of fractures on enhancing the pore system in low-porous reservoirs, core analysis, petrography analysis, and petrophysical measurements are integrated. The study revealed that the Upper Nubian Member is a very heterogeneous reservoir with major lateral and vertical quality variations, and has low porosity and fair permeability. The reservoir can be subdivided into seven lithofacies and grouped into four dominant facies associations (FAs) (i.e., flood plain, crevasse splay, meandering channel, and braided channel) based on sedimentological analysis. Analysis of various lithofacies associations within the fluvial environment indicates that the fluvial meandering and braided channel sandstones exhibit superior reservoir quality. In contrast, the crevasse splay lithofacies associations demonstrate moderate reservoir quality, whereas the flood plain lithofacies association, as anticipated, showcases the poorest reservoir quality owing to its high detrital clay content. The examination of facies, petrography, and routine

core analysis (RCAL) data indicated that mechanical compaction, quartz overgrowth, and clay cement precipitation are the primary factors influencing the deterioration of reservoir quality, whereas feldspar and anhydrite dissolution, along with fractures, contributed to the improvement of reservoir quality. The analysis of fracture characteristics and image logs demonstrated the substantial impact of fractures on the permeability of low-porosity fluvial sediments, with five predominant fracture types shaping the fracture network within the reservoir under investigation. The study delineates the source of fractures and their impact on fluid migration, fluid flow, and the improvement of reservoir quality. It also illustrates the function of fractures as pathways through the less porous sand units. Additionally, it offers guidance and insight for reservoir development in the quest for high-quality sweet spots in low-porosity fluvial reservoirs.

**Keywords:** Fluvial sandstone; Facies analysis; Nubian Formation; Sirt Basin; Libya.

## تقييم التكوينات في تكوين النوبين السفلي من العصر الطباشيري، حوض سرت الشرقي، ليبيا

منى محمد المرغني، عبد الهادي السنوسي خليفة

كلية التقنية الهندسية جنزور

### الملخص

من الضروري الحصول على فهم أعمق للعوامل التي تؤثر على جودة المكامن في المكامن غير المسامية ذات التباين العالي، وذلك لأغراض استكشاف وإنتاج النفط. تتناول هذه الدراسة التأثيرات الترسيبية وما بعد الترسيب على جودة مكامن الرمل الحجري في الجزء العلوي النوبي في حقل شمال جالو، حوض سرت الشرقي، ليبيا. لاستكشاف العلاقة بين الطبقات والعوامل البتروفيزيائية ولتحديد تأثير الشقوق على

تعزيز نظام المسام في المكامن ذات المسامية المنخفضة، يتم دمج تحليل العينات الأساسية، وتحليل البتروغرافيا، والقياسات البتروفيزيائية. أظهرت الدراسة أن الجزء النوبي العلوي هو مكمّن متنوع للغاية مع اختلافات كبيرة في الجودة أفقياً ورأسياً، ويتميز بانخفاض المسامية ونفاذية متوسطة. يمكن تقسيم المكمّن إلى سبع طبقات وتجميعها في أربع مجموعات طبقية سائدة (أي، سهل الفيضانات، انسياب الفيضانات، قناة متعرجة، وقناة مضفرة) استناداً إلى التحليل الرسوبي. تشير تحليل المجموعات الطبقيّة المختلفة للطبقات الصخرية ضمن البيئة النهرية إلى أن الرمال في القنوات المتعرجة والمتشابكة تتمتع بجودة مكمّن أفضل. على النقيض من ذلك، تُظهر تجمعات الليثوفاسيات الخاصة بالشقوق المتفرعة جودة مكمّن معتدلة، بينما تُظهر تجمعات الليثوفاسيات الخاصة بالسهل الفيضاني، كما كان متوقعاً، أسوأ جودة مكمّن بسبب محتواها العالي من الطين الحطامي. أظهرت دراسة الطبقات، والبتروغرافيا، وبيانات تحليل اللب النمطي (RCAL) أن الانضغاط الميكانيكي، ونمو الكوارتز، وترسيب الأسمنت الطيني هي العوامل الرئيسية التي تؤثر على تدهور جودة المكمّن، في حين أن ذوبان الفلسبار والأنهدريت، بالإضافة إلى الشقوق، ساهمت في تحسين جودة المكمّن. أظهرت تحليل خصائص الكسور وسجلات الصور التأثير الكبير للكسور على نفاذية الرواسب النهرية ذات المسامية المنخفضة، حيث شكلت خمسة أنواع رئيسية من الكسور الشبكة الكسرية داخل الخزان قيد الدراسة. تحدد الدراسة مصدر الكسور وتأثيرها على هجرة السوائل، وتدفق السوائل، وتحسين جودة المكمّن. كما يوضح أيضاً وظيفة الكسور كمسارات عبر وحدات الرمل الأقل مسامية. بالإضافة إلى ذلك، فإنه يقدم إرشادات ورؤى لتطوير المكامن في السعي للعثور على نقاط مهمة عالية الجودة في المكامن النهرية ذات المسامية المنخفضة.

**الكلمات الرئيسية:** رمليّة نهرية؛ تحليل الطبقات؛ التكوين النوبي؛ حوض سرت؛ ليبيا

## 1. Introduction

The North Gialo field was discovered in 2002 by the Waha Oil Company, and it is considered to be one of the largest oil discoveries in terms of reserves in Libya in the new century, with about 5 BBOIP (about 1 BBO recoverable reserve). The main hydrocarbon (HC) bearing level is the upper unit of the Lower Cretaceous Nubian Formation (known as Upper Nubian sand). The field is located on the east–west trending horst block in the western part of the Hameimat trough in Sirt Basin, adjacent to the giant field Gialo, E-59 (Figure 1). Sixteen wells have been drilled in the field so far. According to the IHS annual report in 2014, the field was planned to be put into production by 2012 at a rate of 100,000 BOPD and 200 million standard cubic feet per day (MMscf/d) as produced gas being reinjected into the reservoir, but due to the unrest in Libya in 2011, this plan was never carried out.

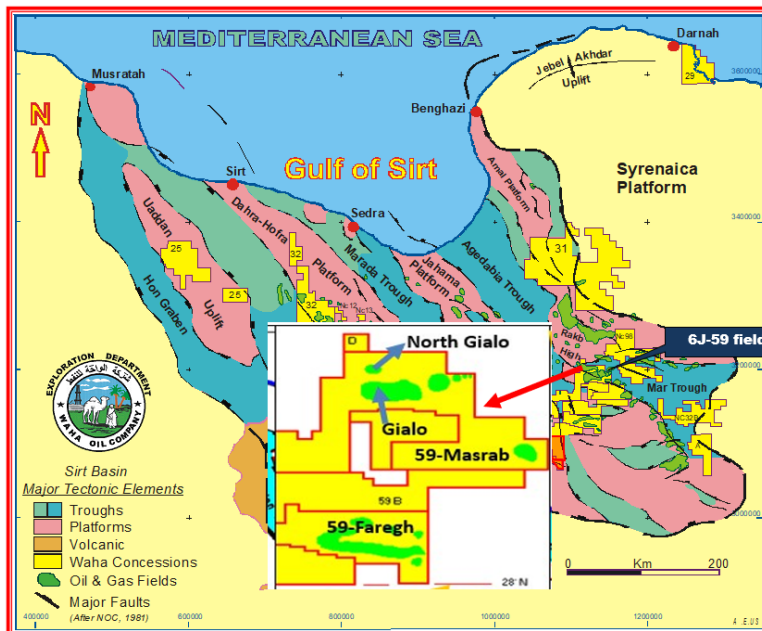


Figure 1. North Gialo (6J-59) field location.

Despite the fact that 16 wells have been drilled in the discovered location, the reservoir characterization of the Upper Nubian sand is still poorly studied. This has been one of the main uncertainties in field development. This study aims to present a detailed geological description of the Nubian reservoir in North Gialo field. This includes the areal distribution of the Upper Nubian sand within the field, a description of the rock facies, rock typing (RT) and HFU identification and their relation to the lithofacies, an evaluation of petrophysical properties, and the distribution of vertical and lateral reservoir quality and the main factors controlling them. This description should contribute to predictions of reservoir quality distribution in the field, thereby reducing the uncertainty in the planning and development of future wells.

## 2. Geology of the Nubian Formation in East Sirt Basin

The Nubian Formation in the southeastern part of Sirt Basin is the most important reservoir in terms of volume of recoverable and remaining hydrocarbon resources [15]. Some of the largest fields in East Sirt Basin, such as Bu Attifel, Sarir (065-C), and Messla, have the Nubian Formation as their main reservoir, which is the only HC-bearing reservoir in the North Gialo field among all the oil wells.

The Nubian Formation comprises an early syn-rift sequence of Lower Cretaceous age, unconformably underlain by granitic basement, igneous extrusions, or Gergaf sandstone (Cambro-Ordovician) and overlain by Upper Cretaceous Formations of mainly marine carbonates ranging in age from Cenomanian to Maastrichtian [4].

The Nubian Formation subdivided into three units: Lower sandstone, Middle Shale, and Upper sandstone units (Figure 2). In most cases, the Upper Nubian is the HC-bearing interval, but occasionally both the Upper and Lower Nubian are productive, as in the Rimal field [9].

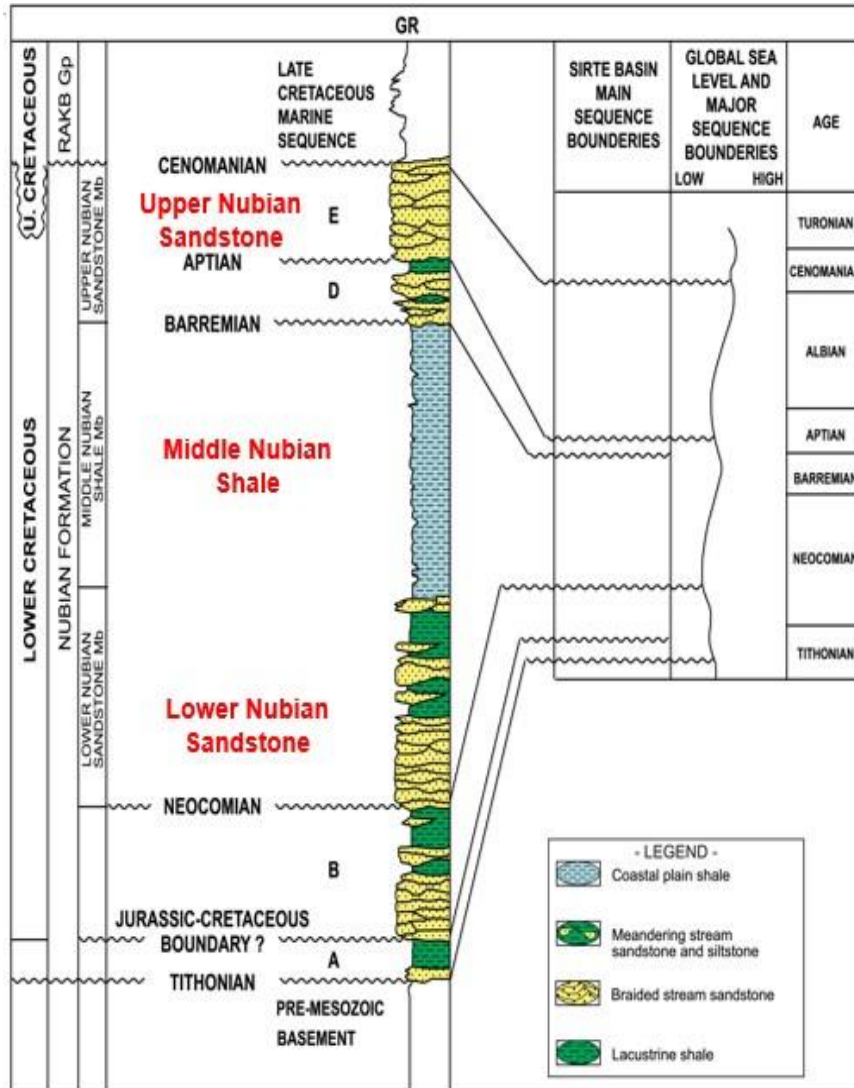


Figure 2. Ages and vertical facies associations: Nubian Fm, Hamaimat Trough, East Sirt Basin [7].

The sedimentological analysis of the Nubian Formation in East Sirt Basin indicates that the Lower Nubian unit was deposited in a braided river system with evidence of a high rate of sediment supply and syn-tectonic deposition. The source of the sediments is

likely to be the adjacent basement highs, such as the Gialo high [10].

The shale facies of the Middle Nubian unit indicate deposition in a low-energy lacustrine, lagoon, or swamp environment [10]. This shale is considered to be a major source rock in Hameimat Trough, as it is very rich in organic material [11]. Geochemical analysis revealed that the Middle Nubian shale unit is the source rock for the Bu Attifel, Nakla, and Tuama fields [6]. This unit laterally changes into a sand unit toward the western part of Sirt Basin [10]. In the Hameimat Trough, the Upper Nubian unit represents alluvial-plain and meander-belt features at some distance from the shoreline [10].

### 3. Database and Methodology

The core description and core images were available for wells 6J2 and 6J16, thus were used to determine the lithofacies and facies associations (FAs). The FAs were coupled with petrographic analysis to determine the depositional system process and environment, and also to understand the diagenetic history of the Upper Nubian unit.

The RCAL reports were available for 4 wells, 6J3, 6J10, 6J12, and 6J16. These were used to determine the reservoir quality, reservoir heterogeneity, relationship between reservoir quality and lithofacies, and main factors controlling the reservoir quality. The RCAL results were used build a relationship between reservoir porosity and Kh through the rock typing process in order to estimate the Kh in the non-core intervals. The rock typing method used in this study was the flow zone indicator (FZI) due to the availability of the RCAL results. Each distinct reservoir unit has unique FZI, reservoir quality index (RQI), and normalized porosity index (NPI) values. FZI is based on the calculation of two terms, RQI and NPI, defined as follows:

$$RQI = 0.0314 * \sqrt{K/\Phi} \quad (1)$$

$$NPI = \Phi/(1-\Phi) \quad (2)$$



$$FZI = RQI/NPI \quad (3)$$

where  $K_h$  is horizontal permeability (mD) and  $\Phi$  is porosity (fraction), and RQI and FZI are in  $\mu\text{m}$  [2].

The RQI and NPI values are used to determine the FZI, which is used to quantify a reservoir's flow nature and build a relationship between petrophysical properties at micro scale (core plugs) and macro scale (well logs) [2]. The porosity and  $K_h$  cross-plot, grouped based on the FZI, was used to subdivide the reservoir into HFUs and group them into GHEs. This was done by using Rocktyper 2018 software.

FE of the Nubian sandstone members was conducted on seven wells in the North Gialo oil field by using wireline logs (for all seven wells) in order to estimate the shale volume ( $V_{sh}$ ), porosity ( $\phi$ ), water saturation ( $S_w$ ), reservoir thickness, net pay thickness, and net reservoir thickness to gross thickness ratio (NtG). The equations used in this study are described in Table 1. The cut-offs used in this work are 35%  $V_{sh}$ , 65%  $S_w$ , and 7%  $\phi$  (provided by the operator). The available wireline logs in all wells underwent quality control (QC) checks. The borehole stability across the Nubian reservoir was checked by using the caliper log in order to ensure that the logs were not affected by washouts (borehole enlargement due to caving). Washout usually negatively affects well log measurements and causes the logging tools to be situated farther from the formation. The distance between the logging tools and the formation is occupied by the drilling mud; therefore, the tool would be more affected by the physical properties of the drilling mud [5]. The larger the washout, the less reliable the logging tool response. For instance, density log measurements decrease with increased washout, which results in increased calculated porosity from the density log [14].

The depths of the Nubian units were available only for well 6J16. In order to determine the depths of the Nubian units in the other wells, well-to-well correlation was carried out by using Petrel 2015 [18]. The correlation was acquired by using gamma ray (GR), sonic ( $\Delta t$ ), density ( $\rho_b$ ), and neutron (NPHI) curves. Based on the available data, the Lower Nubian unit was penetrated in only one



well (B1). For this reason, this work focuses mainly on the Upper Nubian unit. The lithology components of the Nubian Formation were investigated by using DIA porosity density–neutron cross-plots. The intervals used to determine the lithology are only the non-shale intervals (intervals that pass the  $V_{sh}$  cut-off); this is in order to eliminate the impact of  $V_{sh}$  on the cross-plot[1].

The dominant clay type in the reservoir was determined by the potassium–thorium cross-plot. The Archie equation was the first equation to calculate the formation  $S_w$  in clean sandstones and carbonate rocks. In case of shaly rocks with a considerable volume of clay, the Archie model overestimates  $S_w$  [3]. Other equations consider the impact of  $V_{sh}$  on the rock resistivity [10].

In this study,  $S_w$  was computed using the Indonesia equation, as the Nubian reservoir is a shaly sandstone reservoir[13]. The 3D deterministic volume calculation method was used to estimate the stock tank oil initial in place (STOIIP) and ultimate recovery (UR) of the North Gialo field at the Upper Nubian unit. The surface-based volume calculation process in Petrel 2015 software was used to carry out the calculations. The inputs of this process are depth structural maps and the outputs of the petrophysical analysis include the net-to-gross map, net pay average porosity map, and net pay average  $S_w$  map. The variable  $A$  used in the calculation represents the area of the wells used in this study. The OWC used in this study is 12,485 ft-ss. Table 1 includes the equations used for volume calculation.

**Table 1. Equations and methods used in petrophysical analysis of Nubian units of North Gialo Field.**

| Calculation      |                                                        | Equations of calculation and methods                                                                                                                                 | Refrance Number           |
|------------------|--------------------------------------------------------|----------------------------------------------------------------------------------------------------------------------------------------------------------------------|---------------------------|
| Vsh              |                                                        | $I_{GR} = (GR_{log} - GR_{min}) / (GR_{max} - GR_{min})$                                                                                                             | (Atlas, 1979)             |
|                  |                                                        | $Vsh = [0.083 \times (2^{(3.7 \cdot I_{GR})} - 1)]$                                                                                                                  |                           |
| Porosity         | Total                                                  | $\phi_D = (\rho_{ma} - \rho_b) / (\rho_{ma} - \rho_f)$                                                                                                               | (Asquith & Gibson, 1982)  |
|                  |                                                        | $\phi_{ND} = [(\phi_N^2 + \phi_D^2) / 2]^{0.5}$                                                                                                                      |                           |
|                  | Effective                                              | $\phi_{Dcor} = \phi_D - [(\phi_{Dsh} / 0.45) \times 0.13 \times Vsh]$                                                                                                | (Schlumberger, 1975)      |
|                  |                                                        | $\phi_{Ncor} = \phi_N - [(\phi_{Nsh} / 0.45) \times 0.3 \times Vsh]$                                                                                                 |                           |
|                  | $\phi_e = [(\phi_{Ncor}^2 + \phi_{Dcor}^2) / 2]^{0.5}$ |                                                                                                                                                                      |                           |
| Water Saturation |                                                        | $Sw(\text{Indonsian model}) = [(1/Rt) / ((Vsh^{(1-0.5Vsh)} / Rsh^{0.5}) + (\phi_e^m / aRw^{0.5}))]^{2/n}$                                                            | (Poupon-Leveaux 1971)     |
| Reserve Estimate | Net Pay Thickness (h)                                  | Determined according to the cut off values of Vsh, $\phi_e$ , and Sw                                                                                                 | (El-Bakush & Minas, 2008) |
|                  | OWC Depth                                              | The depth at which the Sw becomes above the cut off (65%)                                                                                                            |                           |
|                  | Volumetrics                                            | $HPV = h \times \phi \times (1 - Sw)$<br>$STOIP = (A \times HPV \times 7758) / \beta_o$ ( $\beta_o = 1.6 \text{ RB/STB}$ )<br>$UR = STOIP \times RF$ ( $RF = 25\%$ ) |                           |

$I_{GR}$  = gamma ray index;  $GR_{log}$ =gamma ray reading (API);  $GR_{min}$ =minimum reading clean sandstone or limestone (API);  $GR_{max}$ =maximum reading shale;  $Vsh$ =shale volume.

$\phi_D$ = density porosity;  $\rho_{ma}$ =matrix index used as 2.65 for sandstone lithology;  $\rho_b$ =bulk density (gm/cc(log));  $\rho_f$ =drilling fluid density was oil base mud (0.85gm/cc);  
 $\phi_{Dcor}$ =corrected density porosity;  $\phi_D$ =density porosity;  $\phi_{Dsh}$ =density porosity for shale;  $\phi_{Ncor}$ =corrected neutron porosity;  $\phi_N$ =neutron porosity(log);  $\phi_{Nsh}$ = neutron porosity for shale;  $\phi_e$ = effective total porosity.

$Sw$ = Water saturation,  $Rt$ =deep induction resistivity curve ( $\Omega.m$ );  $m$ =cementation factor (2);  $a$ =tortuosity factor (1);  $n$ = saturation exponent (2);  $Rsh$ = resistivity of shale interval,  $Rw$ =formation water resistivity (provided by the operator as 0.0200 ohm-m at 300 degF).

$HPV$ = Hydrocarbon pore Volume;  $h$ = net pay thickness,  $STOIP$ = stock tank oil Initial In Place;  $UR$ = Ultimate recovery;  $A$ =area in acres;  $\beta_o$ =formation volume factor;  $RF$ =recovery factor;  $7758$ =number of barrels per acre-feet.

**Note:** The variables  $\beta_o$  and  $RF$  were discussed with the operator (Waha Oil Company) and agreed to use the values shown in the table.

#### 4. Upper Nubian Unit Areal Distribution

A depth map of the Upper Nubian unit (Figure 3) derived from the well tops was created to illustrate the lateral extent and continuity of the reservoir across the seven wells, as well as its deepening direction. The map shows that the Upper Nubian is deepening toward the east. The shallowest unit was penetrated at well 6J3 at

10,895 ft ss, whereas the deepest Upper Nubian unit was penetrated at well 6J2 at a depth 12,220 ft ss.

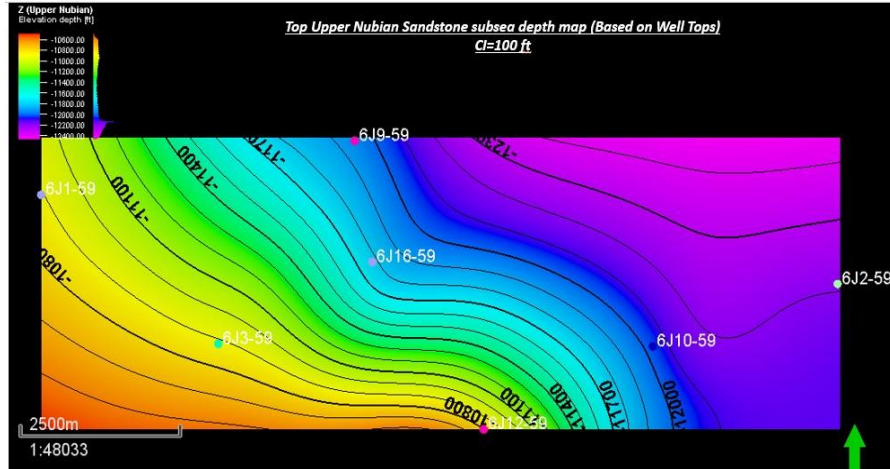


Figure 3. Top Upper Nubian unit subsea depth map based on well data showing deepening toward the E and NE of the study area.

## 5. Lithofacies and Facies Association

A number of lithofacies were identified in the Upper Nubian unit in the 6J16 core and were classified based on the lithology and sedimentary structures. These lithofacies were grouped into five FAs in order to construct a generalized depositional model and to understand the role of the depositional environment in the reservoir quality. The FAs interpreted from the cored wells include meandering fluvial channels (MC), point bars (PB), braided fluvial channels (BC), crevasse splay sands (CS), and overbank deposits (OB). Based on the FA interpretation, the Upper Nubian unit was deposited in a fluvial-dominant environment (braided and meandering systems with associated overbank deposits) (Figure 4).

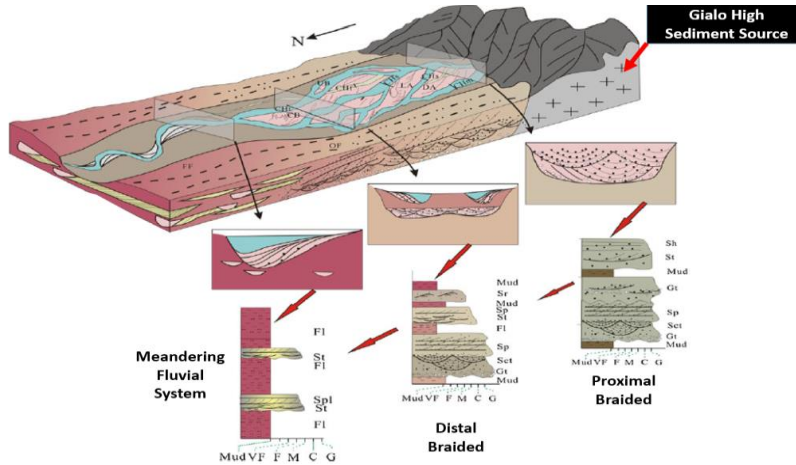


Figure 4. Upper Nubian unit depositional model (after Yao et al., 2018).

The lateral FA continuity across the field was determined by the wireline log correlation, which revealed that the fluvial system covered the entire field area (Figure 5), hence the reservoir architecture was interpreted as amalgamated braided channels and multi-lateral/multi-story meandering channels (Figure 6).

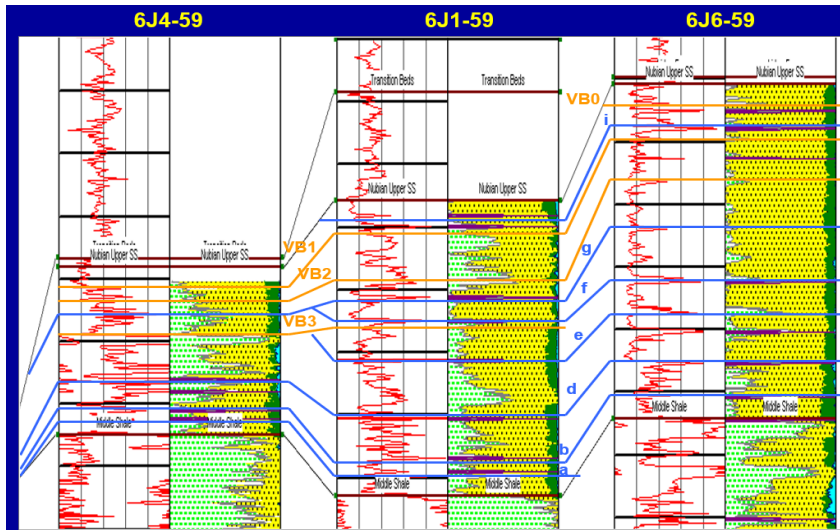


Figure 5. Upper Nubian unit distribution across wells in 6J-59 field.

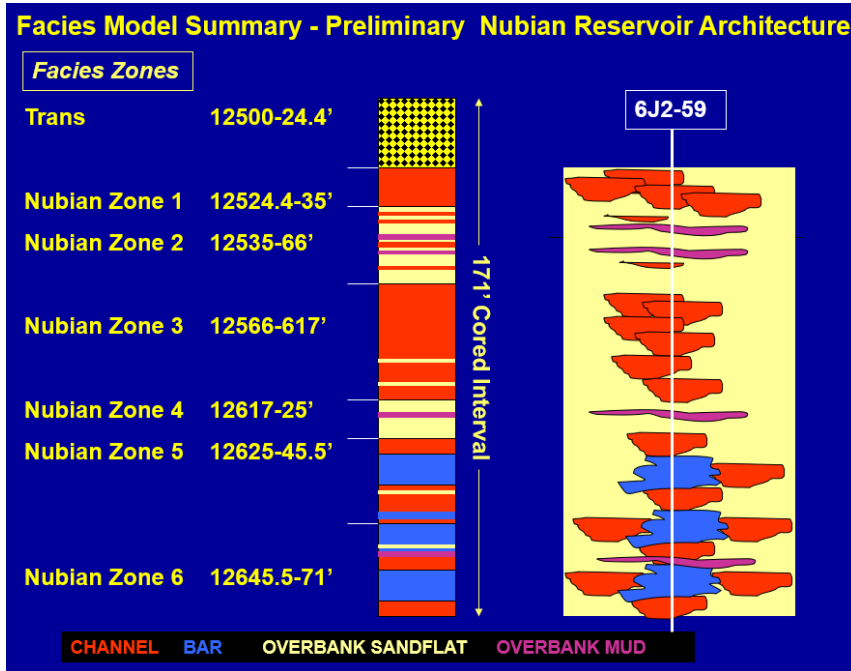


Figure 6. Upper Nubian unit reservoir architecture.

## 6. Results of Petrophysical Analysis

### 6.1. Lithology Identification

The lithology of the Upper Nubian unit in the wells that had no cores available was identified by using the neutron–density cross-plot method. This is the most accurate log analysis method to determine porosity and dual-mineral lithology. The GR cut-off was used to eliminate the shale beds in order to determine the lithology of the non-shale intervals [1]. In most of the studied wells, the majority of points at the Upper Nubian unit are aligned on the sandstone line (sand cluster). Some points formed a cluster directed upward above the sandstone line, which is possibly due to the associated gas effects [17]. The carbonate content and cement at some intervals resulted in some points being plotted on the limestone and dolomite lines [1].

Well 6J16 was used to test the validity of the cross-plot in determining the lithology, because it was the only well with cores

available in this study. A comparison between the lithology discription from the core and the neutron–density cross-plot was carried out. The 6J16 cross-plot at the non-shale intervals of the Upper Nubian unit (blue points) shows that the dominant lithology is sandstone, with most of the points aligned around the sandstone line (Figure 7). The core description at the Upper Nubian unit supports the cross-plot results.

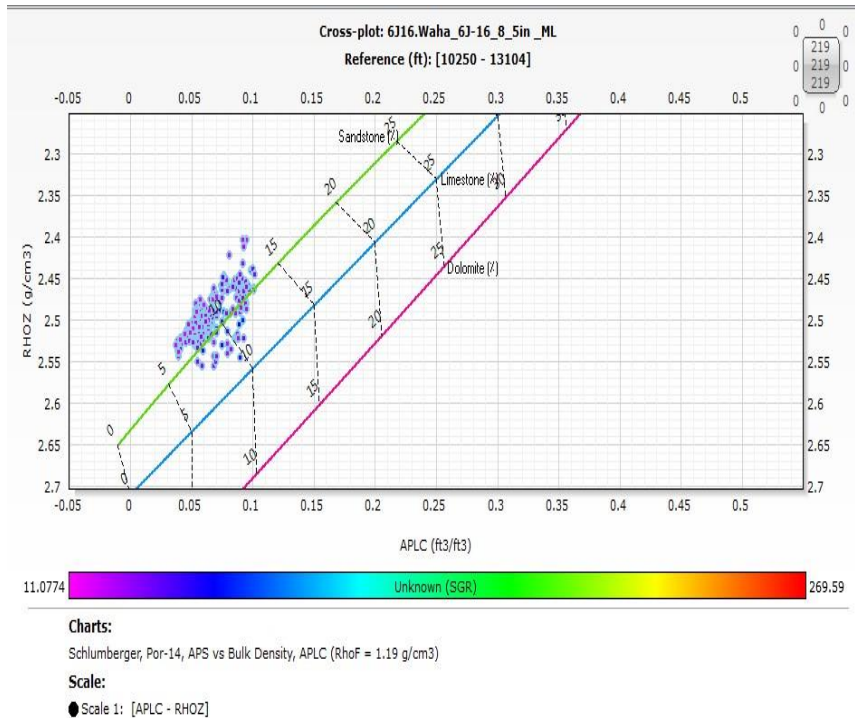


Figure 7. 6J16-59 neutron–density cross-plot of non-shale intervals of Upper Nubian unit. (Green line: sandstone; blue line: limestone; pink line: dolomite). APCL, neutron porosity log corrected to limestone porosity.

The 6J1 well cross-plot of the non-shale intervals of the Upper Nubian unit (blue points) shows that most of the points are aligned in the zone between the sandstone and limestone lines (Figure 8).



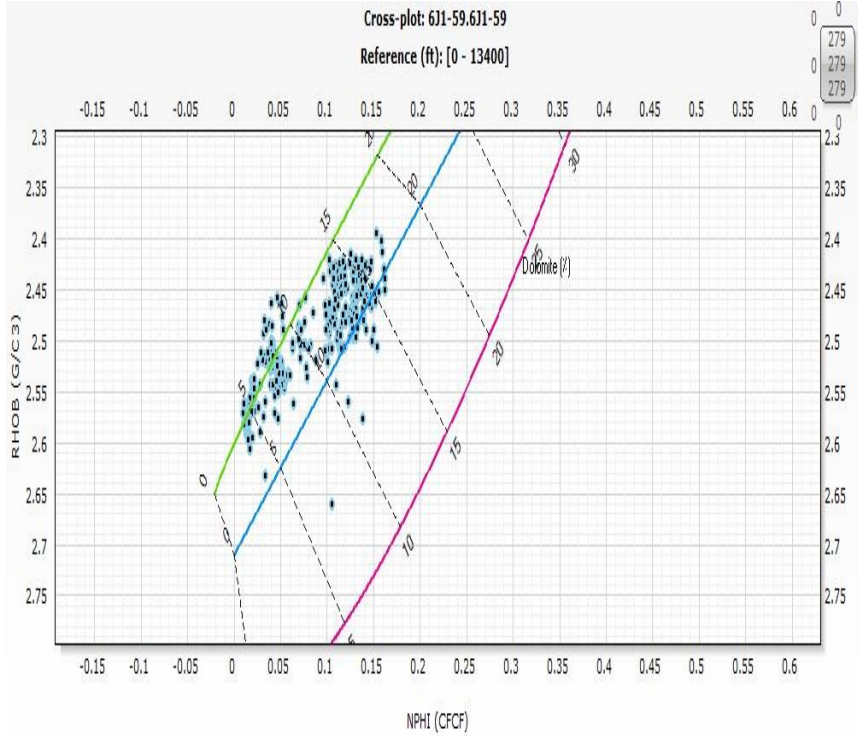


Figure 8. 6J1-59 neutron–density cross-plot of non-shale intervals of Upper Nubian unit. (Green line: sandstone; blue line: limestone; pink line: dolomite).

This might indicate the presence of carbonate cement and/or carbonate content, such as carbonate shells. This interpretation is supported by a micro-paleontological study which concluded that the Upper Nubian unit at well 6J1 includes a significant number of calcareous microfossils, such as benthic and planktonic specimens, foraminifera, and ostracods, and they also used these microfossils to interpret the depositional environment of the Upper Nubian unit as shallow marine deposits (Figure 9)[22].



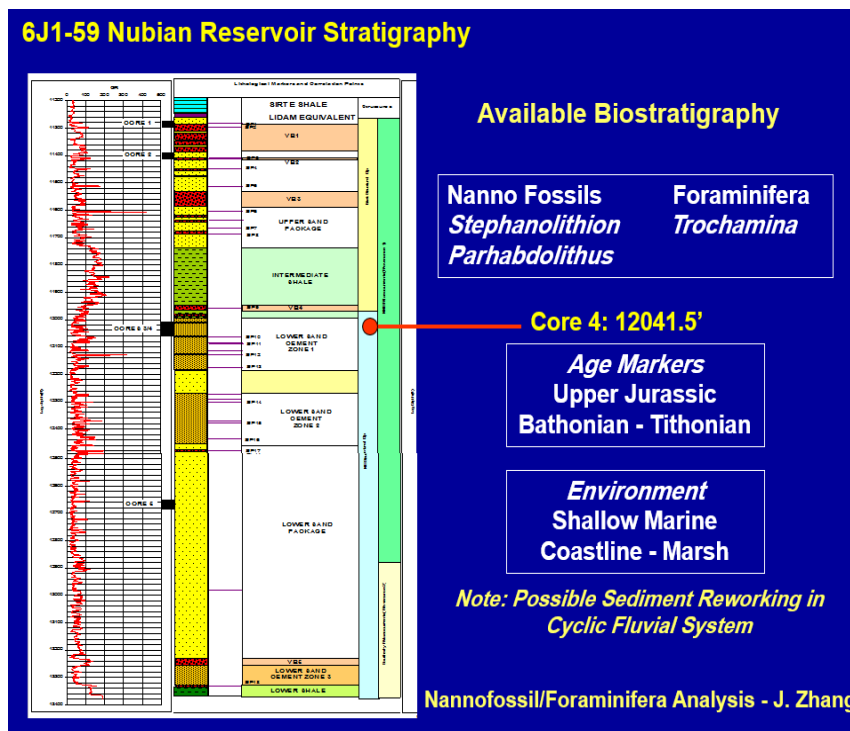
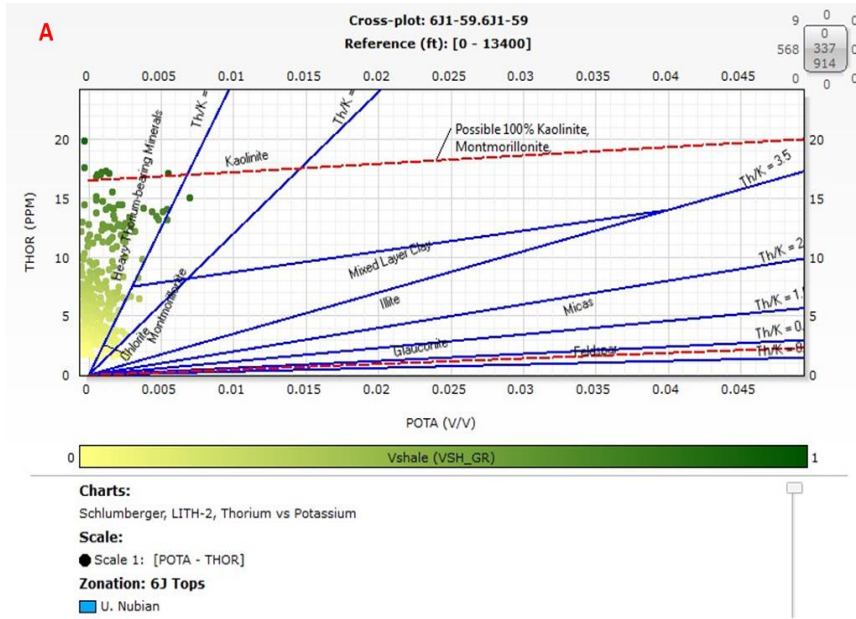


Figure 9. 6J1-59 biostratigraphy analysis results (Zhang et al., 2017).

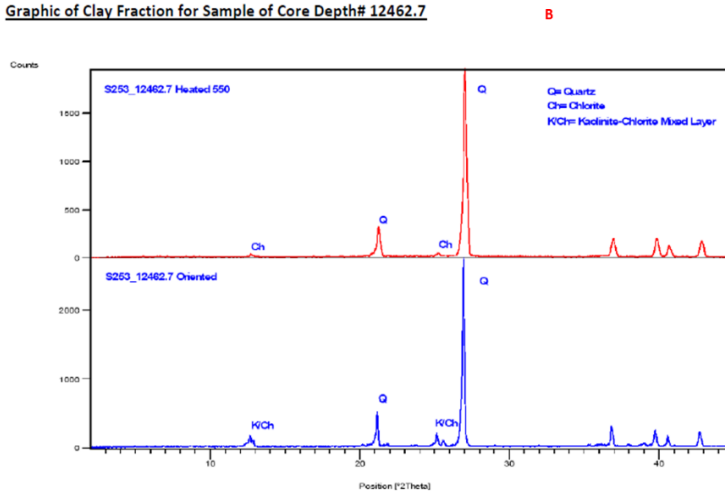
## 6.2. Thorium–Potassium Cross-Plots

The intervals used in the thorium–potassium cross-plot are only the shale intervals (zones with  $V_{sh}$  higher than 35%). In well 6J1 most of the data points concentrate around heavy thorium bearing mineral, with a few points around chlorite (Figure 10A,B). This indicates the limited presence of clay minerals. Instead, the heavy minerals are more abundant. Chlorite is the dominant clay mineral in the Upper Nubian unit at well 6J3 (Figure 11), while in the rest of the wells, the dominant clay minerals are montmorillonite and illite (Figure 12).

تم استلام الورقة بتاريخ: 2024/ 9/ 12 م وتم نشرها على الموقع بتاريخ: 2024/ 10 / 5 م



Graphic of Clay Fraction for Sample of Core Depth# 12462.7



**Qualitative Analysis of the Sample**

| Mineral Name                    | Compound Name             | Chemical Formula    |
|---------------------------------|---------------------------|---------------------|
| Kaolinite- Chlorite Mixed Layer |                           |                     |
| Kaolinite                       | Aluminum Silicate Hydrate | $Al_2Si_2O_5(OH)_4$ |

Figure 10. (A) 6J1-59 thorium–potassium cross-plot shows dominant clay minerals in shale intervals of Upper Nubian unit. (B) XRD results show the presence of chlorite in Upper Nubian unit in 6J1.

تم استلام الورقة بتاريخ: 2024/ 9/ 12 م وتم نشرها على الموقع بتاريخ: 2024/ 10 / 5 م

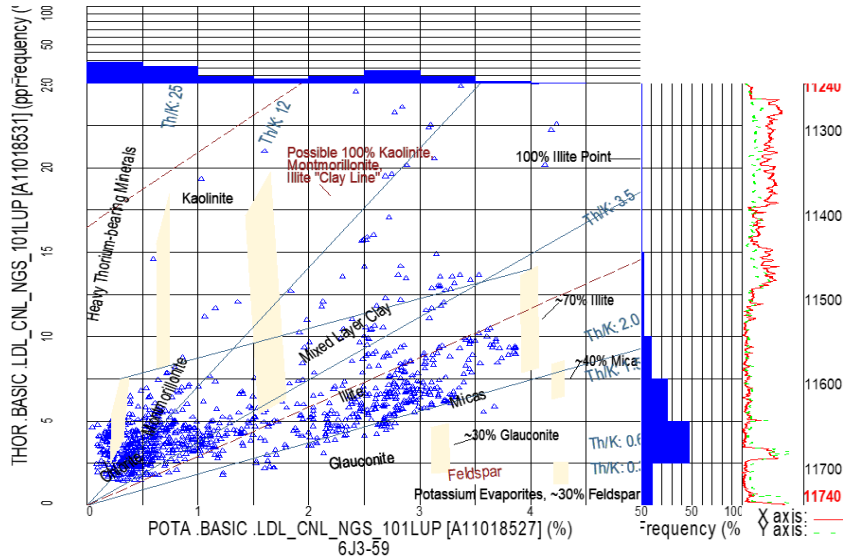


Figure 11. 6J3-59 thorium–potassium cross-plot shows dominant clay minerals in shale intervals of Upper Nubian unit. The blue histograms indicate the frequency distribution of each element on the log curve.

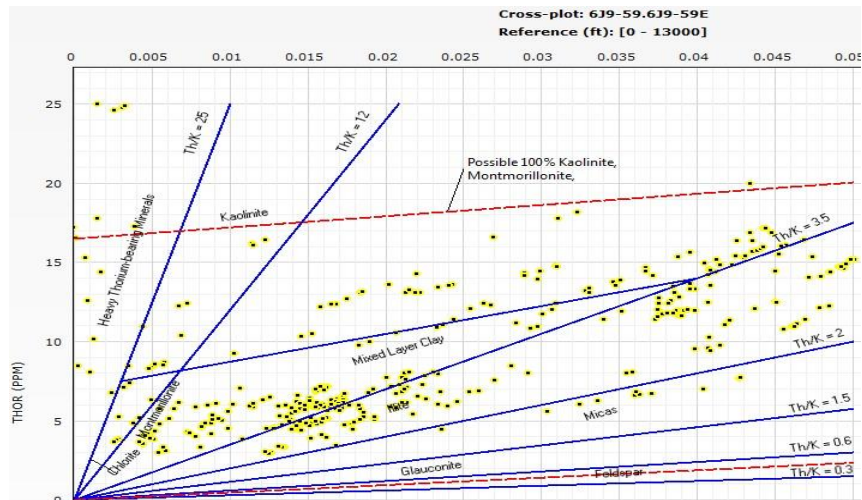


Figure 12. 6J9-59 thorium–potassium cross-plot shows dominant clay minerals in shale intervals of Upper Nubian unit.

### 6.3. Reservoir and Net Pay Determination

The term “gross” is used to refer to the entire section of the Upper Nubian unit, whereas “reservoir” is used for the intervals that pass the  $\phi$  and  $V_{sh}$  cut-offs of  $\geq 7\%$  and  $\leq 35\%$ , respectively. The term “net pay” refers to the reservoir intervals that pass the  $S_w$  cut-off of  $\leq 65\%$ . The gross, reservoir, and net pay thickness and average  $\phi$ ,  $V_{sh}$ , and  $S_w$  for the seven studied wells are shown in Table 2. These results were mapped in order to understand the lateral change in the reservoir characteristics.

**Table 2. Petrophysical results of Upper Nubian unit.**

| Well Name | Top (ft-MD) | Base (ft-MD) | Gross Thickness (ft) | Reservoir Thickness (ft) | Net Pay Thickness (ft) | Net Pay Avg Vsh % | Net Pay $\phi$ % | Net Pay Avg Sw | N:G      |
|-----------|-------------|--------------|----------------------|--------------------------|------------------------|-------------------|------------------|----------------|----------|
| 6J1-59    | 11258       | 11730        | 472                  | 221                      | 173                    | 16                | 11               | 33             | 0.366525 |
| 6J2-59    | 12540       | 12714        | 174                  | 36                       | 26                     | 21                | 10               | 28             | 0.149425 |
| 6J3-59    | 11236       | 11259        | 23                   | 23                       | 23                     | 15                | 13               | 42             | 1        |
| 6J9-59    | 12281       | 12868        | 587                  | 156                      | 127                    | 12                | 8                | 26             | 0.216354 |
| 6J10-59   | 12375       | 12960        | 585                  | 312                      | 188                    | 14                | 7                | 32             | 0.321368 |
| 6J12-59   | 11132       | 11538        | 406                  | 111                      | 107                    | 10                | 9                | 24             | 0.263547 |
| 6J16-59   | 12125       | 12621        | 496                  | 265                      | 210                    | 10                | 10               | 24             | 0.423387 |

### 6.4. Upper Nubian Unit Petrophysical Property Maps

#### 6.4.1. Upper Nubian Unit Thickness Map

The thickness of the Upper Nubian unit was calculated from all wells except well 6J2, as the base of the unit was not reached. The total thickness of the Upper Nubian unit was mapped in order to illustrate lateral thickness change across the field (Figure 13). The thickness map shows significant thinning toward the southwest of the study area, toward Gialo basement high. Well 6J3 penetrated the thinnest Upper Nubian unit at only 23 ft. In this well, the Upper Nubian was underlain by a granitic wash section (older than the Nubian Fm). The Middle and Lower Nubian units were either removed or never deposited as a result of local tectonic movement [11]. In the other wells, the Middle Nubian unit was encountered beneath the Upper Nubian unit. The thinning of the Upper Nubian and the absence of the Middle and Lower Nubian units toward the south indicate that the Gialo basement high affected the deposition

and distribution of the entire Nubian Fm. This interpretation was supported by the absence of the entire Nubian Fm in some wells drilled to the southeast of 6J2, such as 6J5.

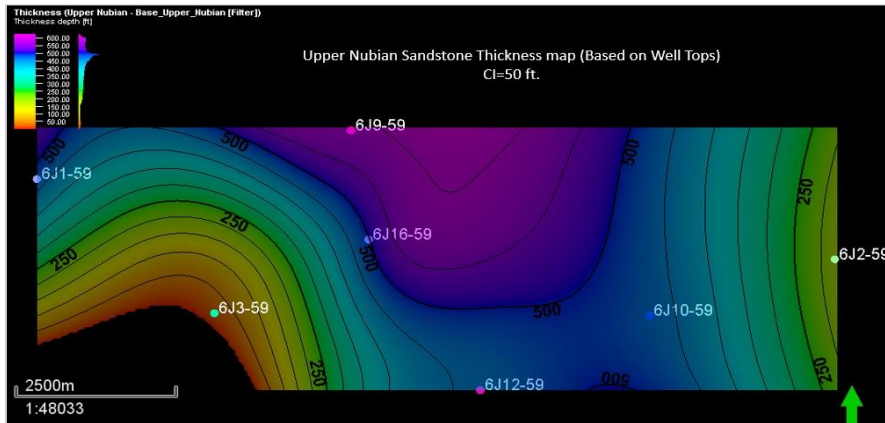


Figure 13. Upper Nubian unit thickness map.

#### 6.4.2. Upper Nubian Unit Lateral Distribution of the $V_{sh}$

The average  $V_{sh}$  for the reservoir interval of the Upper Nubian unit shows a range between 10% (6J12) and 18% (6J2). To the south-central part of the study area, the  $V_{sh}$  map shows that the Upper Nubian unit becomes cleaner (Figure 14), which may indicate a higher-energy depositional environment.

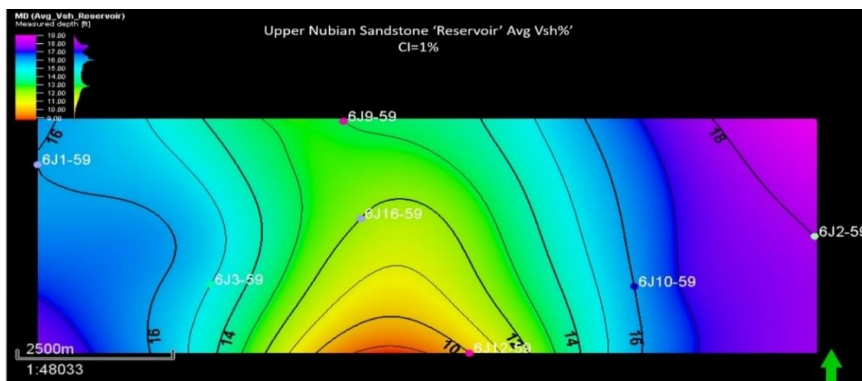


Figure 14. Upper Nubian unit average  $V_{sh}$  for reservoir interval.

### 6.4.3. Upper Nubian Unit Average Porosity Map

Table 2 shows that the average effective porosity of the Upper Nubian unit is poor in most of the wells (5–8%). Well 6J3 is the only well with fair effective porosity (13%). The average effective porosity map (Figure 15) for the reservoir interval shows that the porosity increases toward the southwest along the direction where the thickness of the Upper Nubian unit decreases.

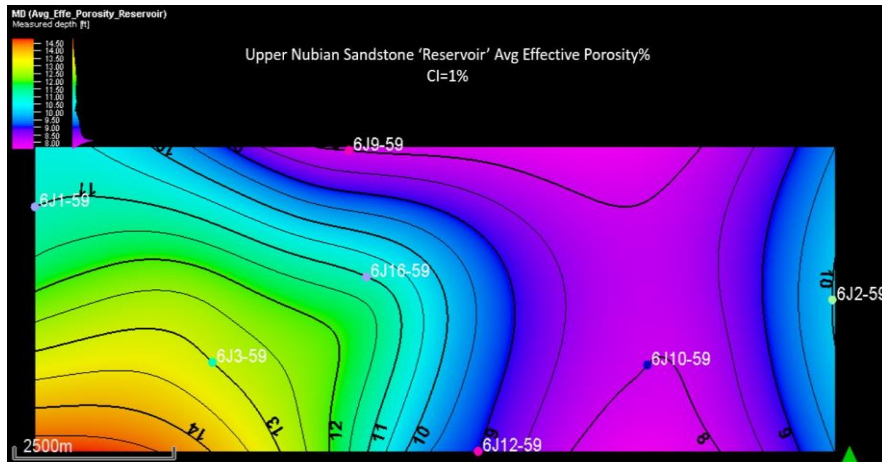


Figure 15. Average effective porosity map of reservoir' interval of Upper Nubian unit.

The low calculated porosity of the Upper Nubian unit does not reflect the high flow rates tested in wells 6J1 (3000 BOPD of 43 API) and 6J12 (2040 BOPD). The high rate of flow in low-porosity reservoirs can only be explained by the presence of considerably increased effective permeability provided by fractures [8]. Fractures usually increase porosity very slightly, but they increase permeability very significantly (Shlumberger Oilfield Glossary, 2021).

### 6.4.4. Reservoir Quality Description

The reservoir core analysis was used to determine the reservoir quality and heterogeneity, calibrate the wireline



log calculated porosity, determine relationship between the reservoir lithofacies and reservoir quality, indicate the flow zone units, and determine the hydraulic units within the reservoir. These should allow us to build a relationship between porosity and permeability, and thus predict the permeability in the non-cored wells. The porosity and permeability measurements were classified based on the LPI standards shown in table 3. The core analysis results revealed that the Upper Nubian unit has a reservoir with low porosity but fair permeability. Core permeability measurements of well 6J16 show that Kh (horizontal permeability) ranges from 0.004–278 mD (but mostly from 1.25–5 mD) (Figure 16). The core porosity ranges from 0.36–20% (but mostly from 6–9%) (Figure 17). The relationship between core porosity and Kh in well 6J16 shows poor correlation (correlation coefficient  $R^2 = 0.22$ ) due to the Kh variation. This variation is likely due to secondary porosity development, such as fractures and dissolution, which likely caused a very subtle increase in porosity but a major increase in permeability (Shulmberger Oilfield Glossary, 2021). The poor relationship between porosity and horizontal permeability makes the calculation of Kh unreliable by using well logs directly; instead, a statistical relationship was established between core permeability and core porosity, such as FZI. In the Upper Nubian unit of well 6J12, the core permeability measurements show that Kh ranges from 0.01–138 mD (but mostly from 0.16–1.25 mD) and the core porosity ranges from 1.47–17.5% (but mostly from 6–10%). The relationship between the porosity and Kh in well 6J12 shows a fair correlation (correlation coefficient



$R^2 = 0.50$ ), which might indicate less contribution of fracture to reservoir permeability (Figure 18).

**Table 3. Standard porosity and permeability categories (after an unpublished LPI report, 2016).**

| Category   | Porosity % | K, mD    |
|------------|------------|----------|
| Negligible | <5         | <0.1     |
| Poor       | 5-10       | 0.1-1    |
| Fair       | 10-15      | 1-10     |
| Good       | 15-20      | 10-100   |
| Very Good  | 20-25      | 100-1000 |

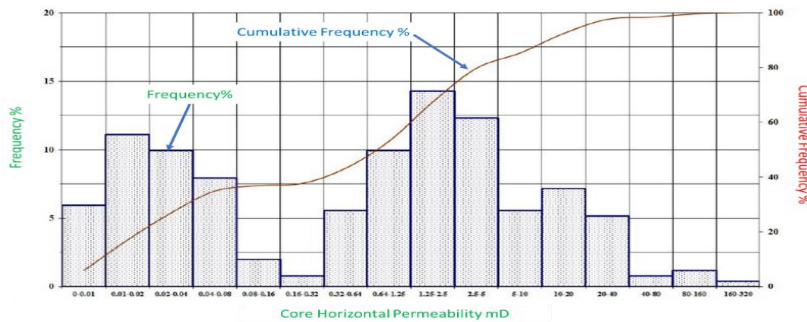


Figure 16. 6J16-59 core horizontal permeability frequency distribution of Upper Nubian unit. (Un-published LPI report, 2016).

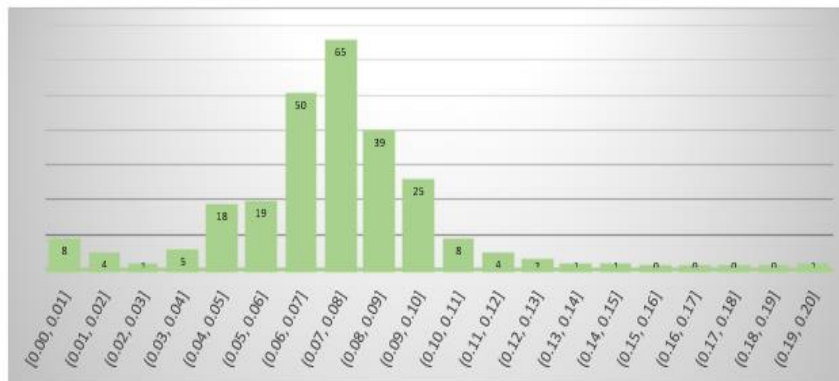


Figure 17. 6J16-59 core porosity frequency distribution of Upper Nubian unit. (Unpublished LPI report, 2016.)

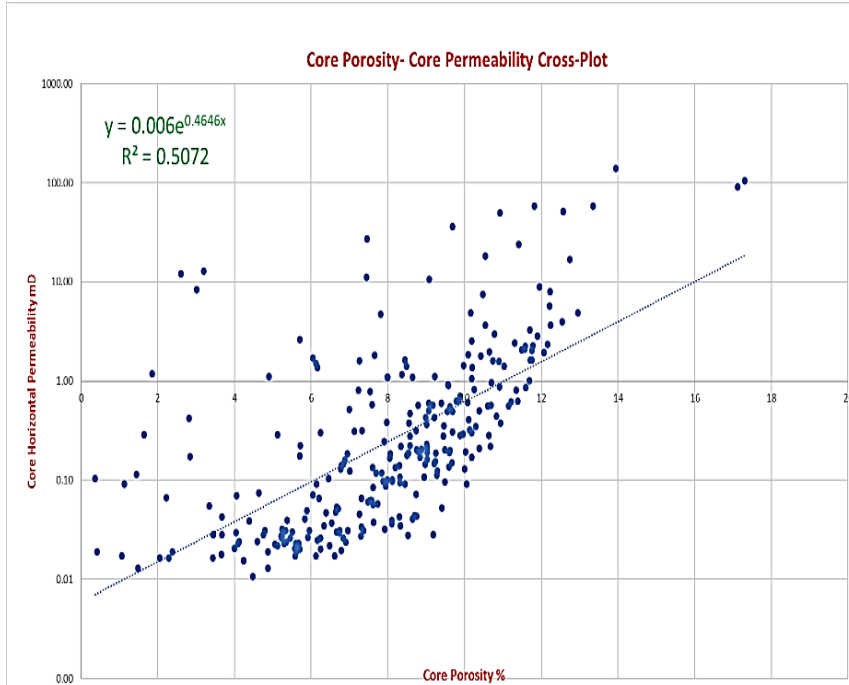


Figure 18. 6J12-69 core Kh vs. core porosity at Upper Nubian unit. (Unpublished LPI report, 2009.)

#### 6.4.5. Reservoir Heterogeneity

Reservoir heterogeneity is an important factor in describing a reservoir; it reflects variations of the reservoir properties in space [19]. Heterogeneity is dependent on the depositional environment and subsequent events, including cementation, compaction, fracture, and dissolution. The ratio of vertical to horizontal permeability ( $K_v/K_h$ ) is one of the reservoir heterogeneity elements and is known as anisotropic permeability [16]. A  $K_h/K_v$  cross-plot of the cored wells revealed variations in the range of heterogeneity in the Upper Nubian reservoir; in well 6J12, the  $K_v/K_h$  correlation coefficient is  $R^2 = 0.0062$  (Figure 19), which indicates high heterogeneity. This is likely related to vertical facies

change (vertical texture change) and compaction. On the other hand, well 6J16 shows much less heterogeneity, with  $R^2 = 0.65$  (Figure 20). Overall, this analysis confirms that the Upper Nubian unit is a heterogeneous reservoir across field 6J-59.

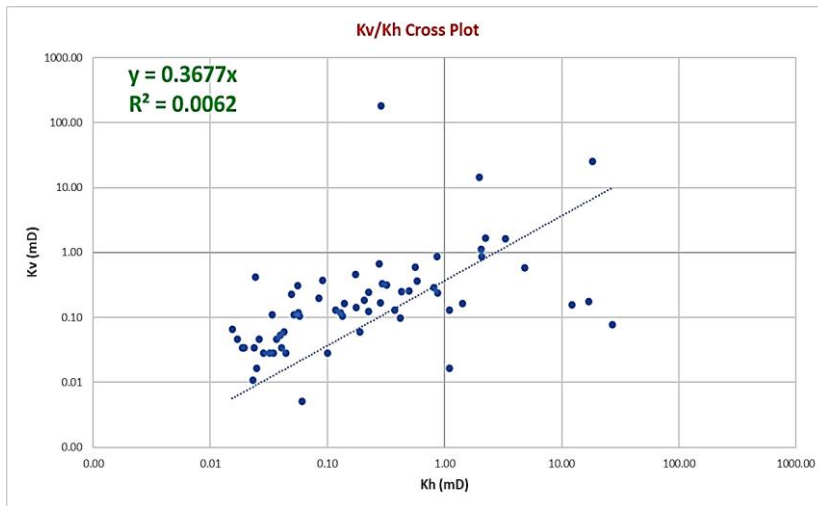


Figure 19. 6J12-59 core Kv/Kh cross-plot of Upper Nubian.

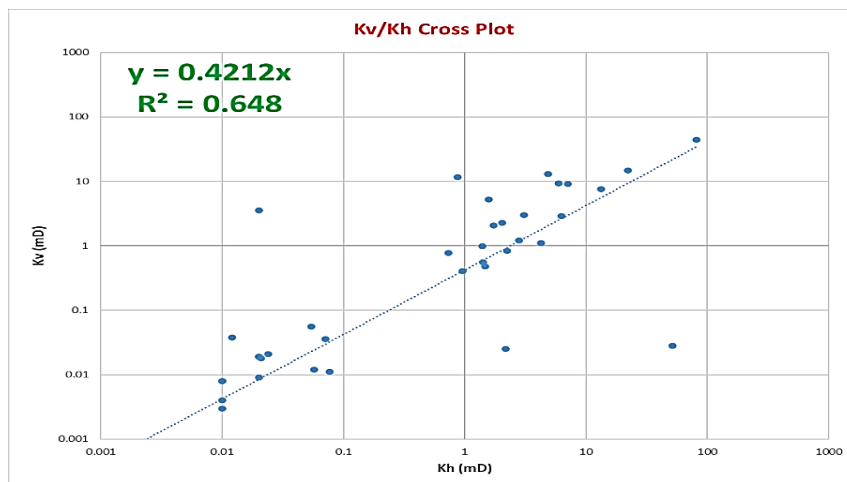


Figure 20. 6J16-59 core Kv/Kh cross-plot of Upper Nubian.

#### 6.4.6. Factors Controlling Reservoir Quality

The relationship between FA, porosity, and permeability of the Upper Nubian unit revealed that the primary textural characteristics of the lithofacies (grain size, sorting, detrital clay content) did not have a significant effect on the distribution of porosity and permeability. The cross-plot shows that the distribution of porosity and Kh is not related to a unique FA, therefore, is not controlled by depositional facies. Three clusters were identified on the cross-plot (Figure 21). The upper cluster samples have fair to good Kh ( $1 \text{ mD} < \text{Kh} < 100 \text{ mD}$ ) and a wide range of porosity values, from poor to fair (4–15%); it also includes all interpreted FAs except overbank (OB) FAs. The thin sections revealed that the main porosity type in this cluster is interparticle and vuggy porosity, resulting from the dissolution of feldspar and/or anhydrite mineral grains. The petrographic analysis concluded that the reservoir quality of this cluster is controlled by texture, dissolution, and possibly fractures. The middle cluster is dominated by MC FAs and shows poor porosity (4–9%) and poor Kh ( $\text{Kh} < 1 \text{ mD}$ ). Thin sections of this cluster reveal that compaction and cementation are the quality controllers, with a very limited contribution by texture. The lower cluster shows the worst reservoir quality, with negligible to poor porosity (3–8%) and negligible permeability ( $< 0.1 \text{ mD}$ ). This cluster mainly reflects the diagenetic impact, including compaction and cementation. Petrographic and scanning electron microscopy (SEM) analysis revealed that the Upper Nubian unit has a chemically “clean” lithology dominated by quartz, with the presence of some anhydrites, but it underwent different post-deposition events that affected its quality (Figure 22). The presence of considerable authigenic clay cement and dissolution porosity may indicate transformation of feldspar mineral and dissolution of anhydrites and/or feldspar.

تم استلام الورقة بتاريخ: 2024/ 9/ 12 م وتم نشرها على الموقع بتاريخ: 2024/ 10 / 5 م

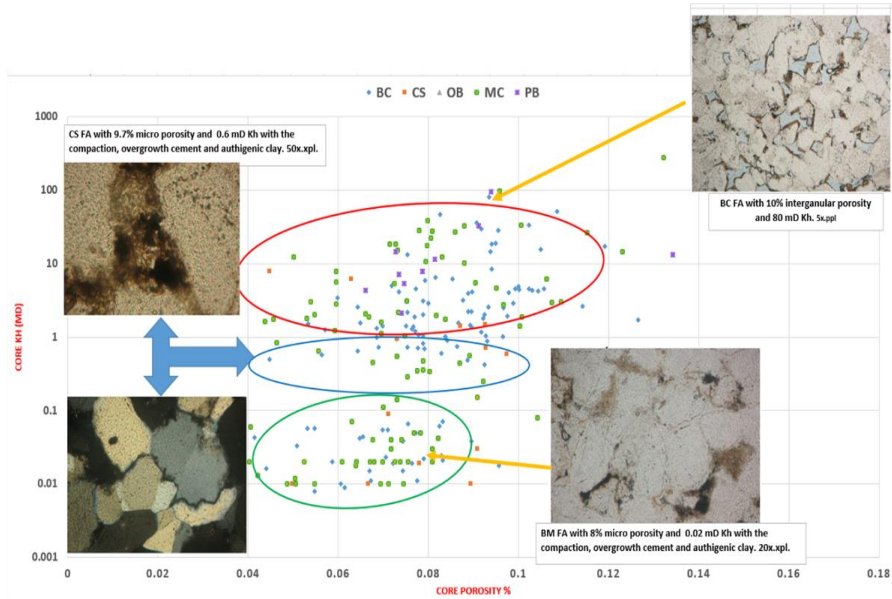


Figure 21. 6J16 core porosity and Kh cross-plot with thin sections representing each cluster.

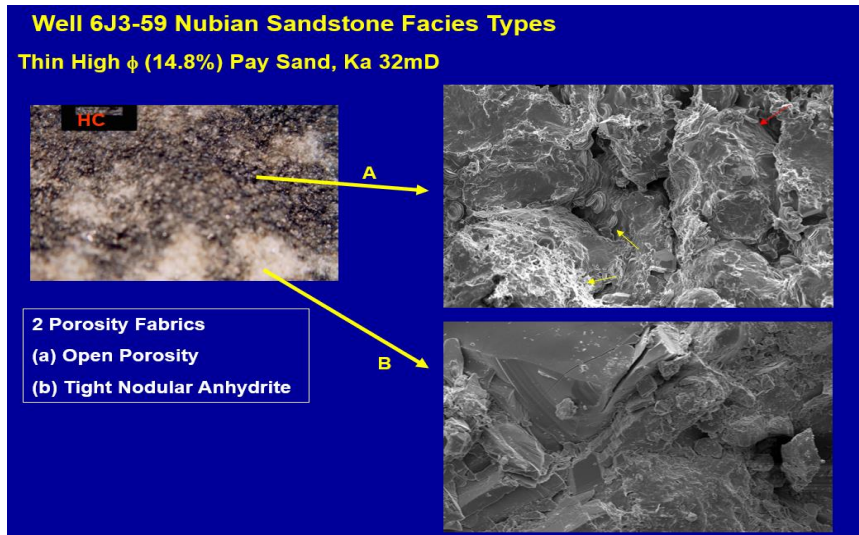


Figure 22. 6J03 SEM showing (A) open porosity, and (B) anhydrite crystals.

On the core scale, fractures seem to have played a significant role in improving the reservoir quality and the oil migration into the reservoir. Figure 23 shows how the fractures worked as a conduit across the tight Upper Nubian sand, which has very poor reservoir matrix properties.

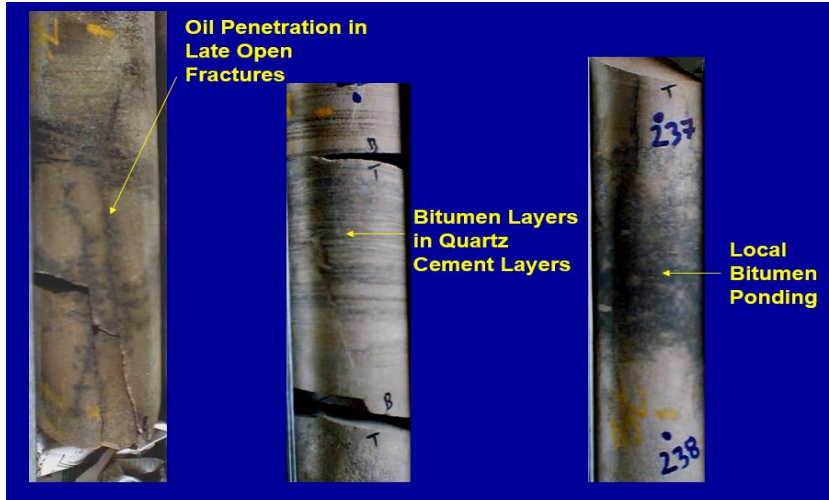


Figure 23. Cores of Upper Nubian sand from 6J3 wells show fracture-controlled oil migration in cemented quartz reservoir sections (tight sand).

The fractures observed in this unit might not have improved the total porosity very much, but they enhanced the permeability, which resulted in high oil flow rates in many 6J wells. Partly open fractures could be interpreted from FMI and UBI logs in some wells (Figure 24), and open fractures could be seen in the core images of well 6J1 (Figure 25).



تم استلام الورقة بتاريخ: 2024/ 9/ 12 م وتم نشرها على الموقع بتاريخ: 2024/ 10 / 5 م

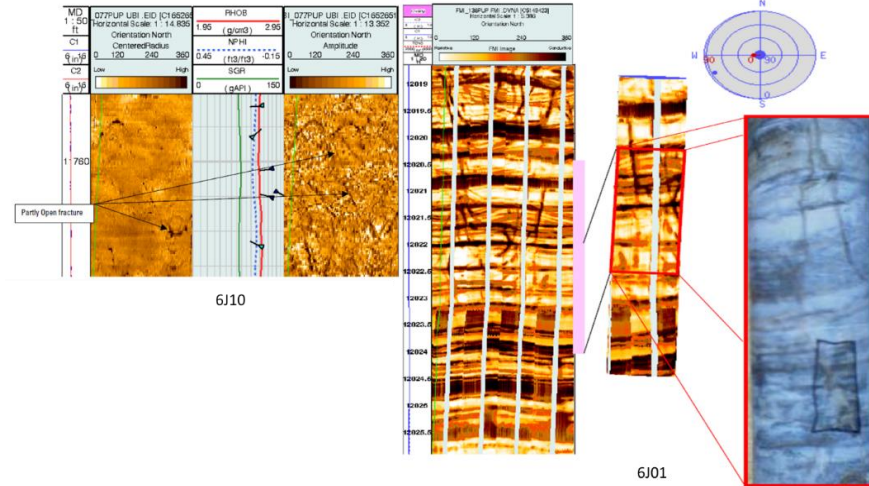


Figure 24. UBI log image from 6J10 at Upper Nubian unit (left) and FMI log image from 6J01-59 partly open fractures.

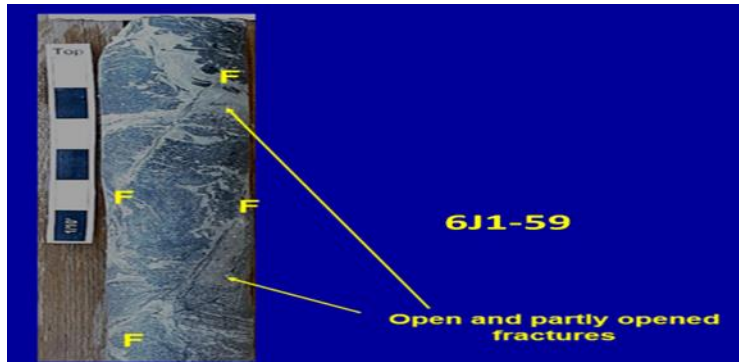


Figure 25. Core photo from Upper Nubian unit at 6J01-59 showing open and partly open fractures.

#### 6.4.7. Upper Nubian Unit Rock Types

Rock typing is a process that is used to subdivide reservoir units into flow units with similar production properties [21]. The main objective of rock typing is to determine as clearly as possible the relationship between geology and petrophysics that can be used to group the reservoir units into geologically and petrophysically



homogeneous units of rocks with a specific distribution and relationship between Kh and porosity. The petrophysical properties within each rock type (RT) must be homogeneous and follow certain geostatistical behaviors (Michel & Bruno, 2014). Rock typing is usually carried out using different methods depending on the available data (Figure 26). In this study, the flow zone indicator (FZI) was used to subdivide the reservoir into HFUs, since the available data were mainly Kh and porosity derived from routine core analysis (RCAL).

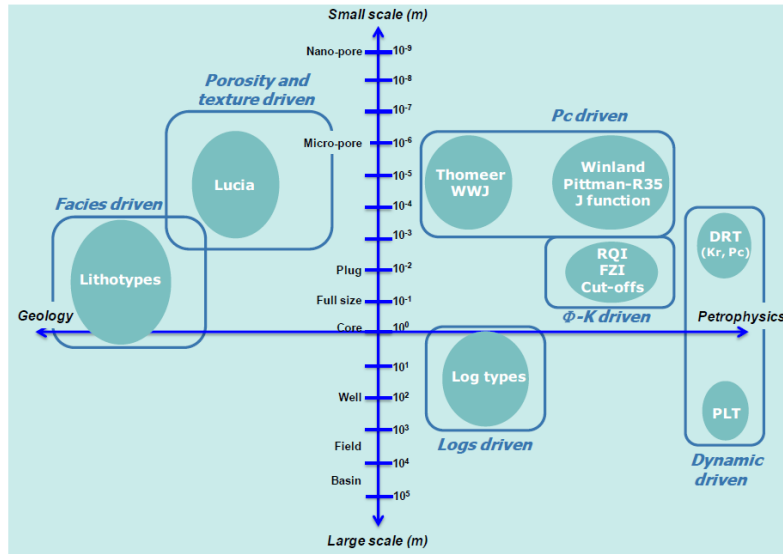


Figure 26. Classification of main rock typing methods. (After Teh and Willhite, 2012.)

The upper Nubian sand unit was subdivided based on a Kh–porosity cross-plot classified by the FZI values into 15 HFUs (Figure 27). The HFUs were grouped into 10 global hydraulic elements (GHEs) to simplify the permeability prediction (Figure 28). There was no direct relation between HFUs and FAs of the Upper Nubian unit, as the same HFU included samples from different FAs. This reflects the heterogeneity of the reservoir. Due to the lack of a relationship between the lithofacies and the rock

تم استلام الورقة بتاريخ: 2024/ 9/ 12 م وتم نشرها على الموقع بتاريخ: 2024/ 10 / 5 م

typing, Kh cannot be predicted by using HFUs or GHEs. In this case, electro-facies must be generated by using different methods such as principal component analysis (PCA). That work is not covered in this paper.

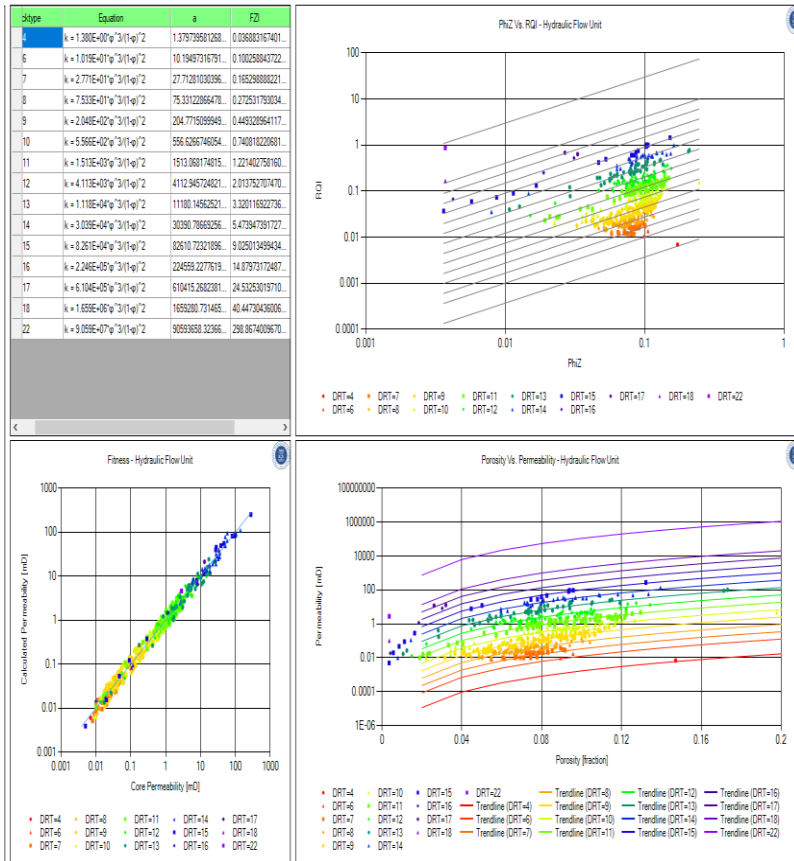


Figure 27. Upper Nubian rock typing (HFUs) in 6J-59 field.

تم استلام الورقة بتاريخ: 2024/ 9/ 12 م وتم نشرها على الموقع بتاريخ: 2024/ 10 / 5 م

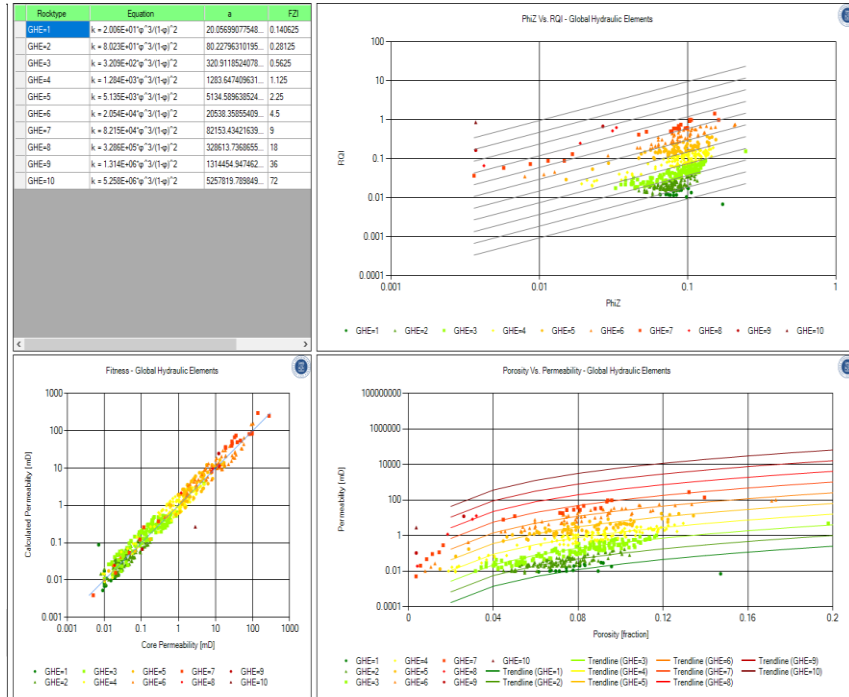


Figure 28. Upper Nubian rock typing (GHEs) in 6J-59 field.

## 6.5. Water Saturation ( $S_w$ ) and Oil–Water Contact (OWC)

The Upper Nubian unit was found to have an oil-bearing reservoir in all wells under study, with  $S_w$  ranging from 24 to 40%. Oil down to (ODT) was found in all wells in the Upper Nubian unit, while OWC could be determined only in well 6J1 in the Lower Nubian unit at a depth of 12,485 ft ss. Although well 6J3 was drilled on the highest part of the structure and penetrated the cleanest sand (low  $V_{sh}$ ) among the wells used in this study, the average  $S_w$  in this well was found to be the highest (40%). This may be because of either the fine-grained sand (high capillary pressure causes high  $S_w$ ) and/or the presence of chlorite clay, which introduces high irreducible water, leading to higher  $S_w$  [20]. The thorium–potassium cross-plot for 6J3 suggests the

presence of chlorite in the Upper unit. However, a petrographic analysis is recommended to confirm the reason for the high  $S_w$ .

## 7. Reserve Estimation

The volume calculations revealed that the STOIP of the North Gialo field at the Upper Nubian unit is 4.14 BBOIP, and with a 25% recovery factor, the UR is calculated to be 1.04 BBO. It is very possible that the STOIP and UR of the North Gialo field are larger than the calculated figures due to underestimation of fracture porosity and permeability.

## 8. Discussion

The Nubian Formation shows thinning toward the southwest of the study area due to the presence of the Gialo paleo/high. This high seems to have affected the thickness and facies distribution of the Upper Nubian unit, where the thinnest and lowest Vsh of the was observed in well 6J3, which is located in the southwestern part of the study area. The lateral change in the e-facies (mainly GR log signature) of the Upper Nubian unit indicates lateral facies change and a possible change in the depositional system, which might have affected the lateral communication among the wells across the reservoir.

Detailed sedimentological, petrographic, and pressure data analyses are highly recommended to understand the reservoir architecture and compartmentalization. The low porosity calculated by the neutron-density logs was found to be close to that of RCAL. This poor reservoir porosity does not reflect the high DST flow rates in wells 6J1 (3000 BOPD) and 6J12 (2040 BOPD), but it might reflect the low flow rate in well 6J9. The high DST flow rates can be explained only by the presence of effective secondary permeability, including vuggy and fracture porosity, whereas the low flow rates indicate a lack of such dual system porosity. The petrographic analysis and RCAL results indicate that the key factors controlling the Upper Nubian reservoir quality degradation in field 6J-59 are mechanical compaction, silica, and clay cements. On the other hand, the dissolved feldspar and/or

anhydrites and the fractures are the main reservoir quality enhancers. The cores clearly illustrate how the fractures worked as conduits across the highly cemented sand units within the Upper Nubian sand (tight intervals). The fractures were observed in the core images and image logs (FMI and UBI).

Lithofacies and core analysis results revealed that the Upper Nubian unit is highly heterogeneous, with changed lateral and vertical reservoir properties. These changes were found to be not related to the rock facies, but more related to the diagenesis process. This reservoir nature was reported from the Rimal field in the Hamaimat trough [15]. Rock typing classification was carried out in order to determine the main reservoir flow units [24]. Fifteen HFUs were identified based on porosity, Kh, and FZI. The lack of a relationship between the lithofacies and the GHEs did not allow use of the rock typing approach to estimate Kh in non-cored wells. Creating an e-facies log by using PCA is highly recommended to define the relationship between the well logs and rock typing [23]. Since the fractures of the Upper Nubian unit made a significant contribution to the oil flow rates, a long-term production test is highly needed to confirm the effective connection between the poor matrix porosity and the open fractures. If the connection between matrix and fracture porosity is limited, the reservoir would have high flow rates for only a very limited time, which would then decline rapidly, and very likely lead to early gas or water breakthrough [12].

## 9. Conclusions

This study illustrates the significance of combining sedimentological, diagenetic, and petrophysical analyses to enhance the understanding and evaluation of the hydrocarbon potential and reservoir quality of the Upper Nubian sandstone reservoir, characterized by low porosity and fair permeability, located in the North Gialo Field of the East Sirt Basin in East Libya. The analysis of sedimentology identified seven lithofacies and four facies associations that characterized the fluvial depositional environment of the North Gialo Field. The sandstone

reservoir in the Upper Nubian Member exhibits low porosity and moderate permeability, as indicated by the petrophysical data obtained from the cores. The sandstones in the Upper Nubian Member exhibit superior reservoir quality in the fluvial meandering and braided channels, with the former showing higher permeability compared to the latter possibly due to improved sorting of sandstone grains and texture. Conversely, the crevasse splay FAs demonstrate moderate reservoir quality, while the flood plain FA presents the lowest reservoir quality in the studied field owing to its elevated detrital clay content. The Upper Nubian Member exhibits a high degree of heterogeneity as indicated by lithofacies and core analysis results. These variations were determined to be more closely associated with the diagenesis process rather than the rock facies. Petrographic analysis and RCAL results point towards compaction and cementation (such as quartz overgrowth and clay precipitation) as the key diagenetic factors influencing the decline in reservoir properties, while the presence of dissolved feldspar and/or anhydrites, along with fractures, led to an improvement in reservoir quality. The fractures identified within this unit may not have significantly increased the overall porosity, but they did improve the permeability, leading to elevated oil flow rates in numerous wells within the field under study. This relatively high production rate is attributed to the existence of substantial secondary porosity, including fractures and vuggy porosity. The research offers a point of comparison for the effects of sedimentology, diagenesis, and petrophysical characteristics on the quality of fluvial sandstone reservoirs. It also sheds light on the factors influencing reservoir quality in low porosity to fair permeability reservoirs, and the significance of fractures in improving reservoir quality. This information can be valuable for field development and in similar geological settings.

## References

- [1]. Shady, A. A., El-Shishtawy, A. M., Hameed, A. A., & AbdelKader, T. (2010). Reservoir characterization of the upper cretaceous Bahariya formation, Khalda ridge, north western desert, Egypt. In Proceedings of the 6th International Symposium on Geophysics, Tanta, Egypt (pp. 34-46).
- [2]. Amaefule, J.O.; Altunbay, M.; Tiab, D.; Kersey, D.G.; Keelan, D.K. Enhanced reservoir description: using core and log data to identify hydraulic flow units and predict permeability in uncored intervals/wells. In Proceedings of the SPE Annual Technical Conference and Exhibition, Houston, TX, USA, 3–6 October 1993; Paper 26436, pp. 205–220.
- [3]. Archie, G.E. The electrical resistivity log as an aid in determining some reservoir characteristics. Trans. AIME 1942, 146, 54–62.
- [4]. Barr, F.T.; Weegar, A.A. Stratigraphic Nomenclature of the Sirte Basin Area, Libya; Petroleum Exploration Society of Libya: 1972.
- [5]. Bassiouni, Z. Theory, Measurement, and Interpretation of Well Logs; Henry, L., Ed.; Doherty Memorial Found of AIME, Society of Petroleum Engineers: Dallas, TX, USA, 1994; 60.
- [6]. Burwood, R.; Redfern, J.; Cope, M. Geochemical evaluation of east Sirte Basin (Libya) petroleum systems and oil provenance. In Petroleum Geology of Africa: New Themes and Developing Technologies; Arthur, T.J., MacGregor, D.S., Cameron, N.R., Eds.; Geological Society, London. Spec. Pub.: 2003; Volume 207, pp. 203–204.
- [7]. Causin, E.; Rossi, E.; Radaelli, F.; El-Ageli, I. Abu Attifel field: gas injection process to improve the final oil recovery. Pet. Res. J. 2002, 14.
- [8]. Crain, E.R. Crain's Petrophysical Handbook; Mindware Ltd.: Westerville, OH, Canada, 2010.
- [10]. El-Hawat, A.; Missallati, A.A.; Bezan, A.M.; Taleb, T.M. The Nubian Sandstone in Sirt Basin and its correlatives. First



- Symposium on the Sedimentary Basins of Libya, Geology of the Sirt Basin; Salem, M.J., El-Hawat, A.S., Sbeta, A.M., Eds.; Elsevier: Amsterdam, The Netherlands, 1996; Volume 2, pp. 3–20.
- [11]. Gonzalez, O. Water Saturation Equations: Archie, Simandoux, Indonesia, Fertl, and SW Ratio. 2012. Available online: <https://geoloil.com/computingSW.php> (accessed on 17 April 2020).
- [12]. Hallet, D. Petroleum Geology of Libya; Elsevier Science B. V.: Amsterdam, The Netherlands, 2002.
- [13]. Nelson, R.A. “Evaluating Fractured Reservoirs: Introduction”, Geologic Analysis of Naturally Fractured Reservoirs, 2nd ed.; Gulf Professional Publishing: Woburn, MA, USA, 2001, pp. 1–2.
- [14]. Poupon, A.; Leveaux, J. Evaluation of Water Saturation in Shaly Formations. In Proceedings of the SPWLA 12th Annual logging symposium, Dallas, TX, USA, 2–5 May 1971; Volume 12, pp. 1–2.
- [15]. Rider, M.H. The Geological Interpretation of Well Logs, 2nd ed.; 2002; ISSN 0-9541906-0-2.
- [16]. Sadeg, E.B.H.; Haithem, M.A. facies and petrophysical analysis of Nubian reservoir, Rimal oil field–Sirte basin. In Proceedings of the Fifth International Conference on the Geology of Africa, Assiut, Egypt, October 2007; Volume 1, pp. vi-51–vi70.
- [17]. Shedid, S. Prediction of vertical permeability and reservoir anisotropy using coring data. J. Pet. Explor. Prod. Technol. 2019, 9, 2139–2143.
- [18]. Schlumberger. Petrel online help, Petrel Introduction Course Schlumberger, 2009, 560p.
- [19]. Schlumberger. Petrel 2015 software platform. 2015.
- [20]. Tavakoli, V. Reservoir Heterogeneity: An Introduction. In Carbonate Reservoir Heterogeneity. Springer Briefs in Petroleum Geoscience & Engineering; Springer: Cham, Switzerland, 2020. [https://doi.org/10.1007/978-3-030-34773-4\\_1](https://doi.org/10.1007/978-3-030-34773-4_1).

- [21]. Tudge, J. Low Resistivity Pay; the Role of Chlorite in Controlling Resistivity Responses. Leicester Research Archive. 2010. Available online: <https://ira.le.ac.uk/bitstream/2381/28359/1/2010TudgeJPhD.pdf> (accessed on).
- [22]. Teh, W.J.; Willhite, G.P. Improved Reservoir Characterization using Petrophysical Classifiers within Electrofacies. In Proceedings of the SPE Improved Oil Recovery Symposium, Tulsa, OK, USA, 14–18 April 2012; p. 154341-pp.
- [23]. Zhang, N.; Dong, G.; Yang, X.; Zuo, X.; Kang, L.; Ren, L.; Liu, H.; Li, H.; Min, R.; Liu, X.; et al. Diet reconstructed from an analysis of plant microfossils in human dental calculus from the Bronze Age site of Shilinggang, southwestern China. *J. Archaeol. Sci.* 2017, 83, 41–48.
- [24]. Porras, J.C.; Campos, N. Rock typing. A key approach for petrophysical characterization and definition of flow units, Santa Barbara field, Eastern Venezuela Basin. In Proceedings of the SPE Latin American and Caribbean petroleum engineering conference, Buenos Aires, Argentina, 25–28 March 2001.